doi.org/10.36721/PJPS.2026.39.5.REG.13335.1

Development of transdermal nanofilm containing fluticasone propionate: *in-vitro, in-vivo* correlation

Muhammad Irfan Siddique*
Department of Pharmaceutics, Faculty of Pharmacy, Northern Border University, Rafha, Saudi Arabia

Abstract: **Background**: Psoriasis is one of the chronic inflammatory skin conditions, affecting about 2-3% of the world population. Steroidal treatment are only best choice of treatments, but it is often associated with side effects due to higher lipophilicity. **Objectives**: In this work, a nanoparticle-loaded transdermal film was developed to maintain nanoparticle integrity in the skin. **Methods**: Fluticasone propionate loaded chitosan nanoparticles (NPs) were developed, and their particle size, zeta potential, drug loading, entrapment efficiency and scanning electron microscope (SEM) images were determined. The NPs-loaded film was further characterized for appearance, thickness and Fourier Transform Infrared (FTIR) spectra, and an *in vitro* and *in vivo* permeation study was conducted. **Results**: The particle size of FSNPs was found to be 250nm with +32.4 ±1.5 mV zeta potential, great entrapment efficiency and spherical in shape. *In vivo* dermato-kinetic studies showed long-term, confined drug release from the NP-formulated film in the epidermal layers, compared with the film containing free drug. **Conclusion**: The study demonstrated that the FSNPs-loaded film showed higher skin permeation, which is effective for managing psoriasis and warrants further evaluation.

Keywords: Chitosan nanoparticles; Fluticasone propionate; *In-vivo* dermatokinetics; Psoriasis

Submitted on 03-09-2024 – Revised on 09-03-2025 – Accepted on 02-07-2025

INTRODUCTION

Psoriasis is a chronic inflammatory skin disease characterized by relapsing episodes of inflammatory lesions and excessive keratinocyte growth and differentiation. The prevalence of this disease is about 2-5% worldwide. Topical (local) therapy is the treatment of choice for mild to moderate psoriasis, but the stratum corneum (SC) acts as a true barrier to localized delivery to the skin. Topically administered drugs, especially glucocorticoids, not only require adequate doses on anticipated areas of the skin but also inhibit the possibility of obnoxious side effects of such potent drugs. In contrast, psoriatic skin requires a high local drug concentration at the target site with minimal systemic absorption. Common side effects of topical glucocorticoids (TGs) include skin atrophy, striae, and irritation. There is always a demand to develop a formulation that helps eliminate side effects. One of the major challenges in developing topical formulations for such inflammatory skin diseases is delivering and maintaining safe, therapeutic drug levels (Try *et al*., 2016). Many conventional therapies are available, but do not provide precise penetration into targeted inflamed areas of the skin (Nutten, 2015).

TGs are still the best treatment option for inflammation, especially psoriasis. Among the TGs, fluticasone propionate is a steroid of class D. TGs show their anti-inflammatory activity employing glucocorticoid-responsive elements (GREs) located in the nucleus; they down-regulate the generation of immunocompetent inflammatory cells and cytokine production, as well as minimizing the number of *Staphylococcus aureus* present at the skin (Almawi and Melemedjian, 2002). TGs like fluticasone propionate are associated with many local as well as systemic side effects. These side effects cause steroid phobia amongst the patients, whereas these effects are minimised by controlling the rate of release and targeted delivery (Korting and Schöllmann, 2012; Ashraf *et al*., 2025).

Researchers have tested many approaches to improve treatment specificity (Parhi *et al*., 2015). NPs have lately gained significant attention due to their size, charge, and high penetration (DeLouise, 2012). It was also found that NPs can penetrate the skin, making them a potential strategy for treating chronic skin inflammation (Abdel-Mottaleb *et al*., 2012).

However, among the polymeric NPs, chitosan (CS) has gained remarkable attention because it is bio-degradable, non-toxic, non-irritant, and bio-active, so CS is a choice of many pharmaceutical and bio-medical products (Pati *et al*., 2011, Yassin *et al*., 2010, Papadimitriou *et al*., 2008). The NH^{3+} and -OH groups present in the CS make it accessible for the chemical reactions (Gan and Wang, 2007). Moreover, various studies have examined CS for its potential application in topical drug delivery systems (Sivakumar *et al*., 2013). Polymeric CS NPs have been shown to modulate drug release from the dosage form, alter the duration of action, and enable targeted delivery to the required area (Illum, 2007). NPs were investigated for their size, zeta potential, and surface morphology.

These polymer NPs are difficult to apply to the skin, so they require some carriers. NPs-loaded films are gaining attention as drug delivery carriers due to their convenience, superiority over conventional semisolid dosage forms, and efficient, less-toxic topical applications (Deb *et al*., 2018). It also has the potential to improve patient compliance by

**Corresponding author:* e-mail: muhammad.siddique@nbu.edu.sa

reducing dosing frequency. In this study, fluticasone propionate loaded with CSNPs was formulated and characterized for its particle size, Zeta potential, and PDI. Then these drug-loaded NPs were incorporated into a sodium alginate and pectin film. The film was prepared using a simple and reproducible solvent-casting method. The film was characterized based on its surface morphology and the interaction between the polymers and drug molecules. Moreover, drug permeation studies were conducted *in-vitro* and *in-vivo* to investigate *in-vitro and in-vivo* correlations of drug molecules (Fluticasone propionate). The correlation was investigated based on the *in-vitro* and *in-vivo* drug permeation study.

MATERIALS AND METHOD

Chemicals

Fluticasone propionate (Sigma Aldrich), Chitosan (LMW) with 9% deacetylation, and Tripolyphosphate (TPP) were bought from Sigma Aldrich. Other laboratory chemicals, like acetone, acetonitrile, and methanol, were of analytical grade. Cellulose membrane filters and dialysis tubing were purchased from Sigma Aldrich. Sodium alginate, pectin, and glycerin were purchased from a licensed local supplier.

Method

Preparation of nanoparticles

The ionic gelation method was used to synthesise Fluticasone propionate-loaded CS NPs (Siddique *et al*., 2015). 5mg of Fluticasone propionate was solubilized in ethanol. Briefly, a 0.5 mg/mL lower-molecular-weight (LMW) chitosan solution was prepared in aqueous acetic acid. Both CS and drug solution were mixed at 500rpm for 15 minutes. A TPP solution at 1mg/ml was prepared separately. 10 mL of TPP solution was added dropwise while stirring at 700rpm on a magnetic stirrer (SCI340 HS) for 30 minutes. Spontaneous generation of polymeric NPs of fluticasone propionate was formed. The solution was placed in an ultracentrifuge (Beckman-Coulter, CA, USA) at 28000 rpm for 45 min. The collected pallets were freeze-dried using Lab1st (USAau-36) for further analysis.

Characterization of nanoparticles

Collected pellets were redispersed in un-ionized water and analysed for particle size, zeta potential, and polydispersity index using a Malvern Zetasizer Nano ZS 1600. The nanosuspension was transferred into a specialized cuvette using a 5-mL syringe at a detection angle of 90°. All samples were analysed in triplicate to generate a mean ± standard deviation (SD). Furthermore, to investigate the surface morphology of CSNPs, SEM samples were prepared by carefully attaching the NPs to a carbon-coated copper grid, then adding 1% ammonium molybdate solution. The samples were dried and further coated with gold and analysed at 50mA for 15s.

Standard calibration curve

10mg of accurately weighed Fluticasone propionate was added to a 100mL volumetric flask, 10mL of acetone was added, and the volume was made up to 100mL with distilled water to prepare a stock solution at 100 µg/mL. Serial dilutions of fluticasone propionate were prepared at 5, 10, 15, 20, and 25 µg/ml by adding acetone to the stock solution. The absorbance of the above-mentioned serial dilution was measured at wavelength λ_{max} of 246 nm against a blank (acetone) (Kulkarni *et al*., 2016). A calibration curve was made, which obeyed Beer's Lambert Law.

Drug loading and entrapment efficiency (%EE)

The NP solution was centrifuged at 12000rpm for 30min. The supernatant solution was recovered and assayed for dissolved Fluticasone propionate by UV spectroscopy (Shimadzu UV-1601, Shimadzu Co., Ltd., Japan) at λ_{max} = 246 nm (Kulkarni *et al*., 2016). This was used to translate the absorbance values attained from the supernatant into a concentration. For each batch, drug loading and entrapment efficiency (%EE) were determined as follows:

$$\text{DL (\%)} = \frac{\text{Mass of entrapped drug}}{\text{Mass of entrapped drug} + \text{Mass of polymer}} \times 100$$

$$EE\ (\%) = 100 - \frac{weight\ of\ drug\ in\ supernant}{initial\ drug\ weight} \times 100$$

Preparation of film

Both fluticasone propionate CSNPs and aqueous gel (Blank) films were formulated using the solution casting method. An equal mass fraction (1:1) of sodium alginate (SA) and pectin (PC) was mixed to prepare the film. Briefly, polymers were dissolved in distilled water containing glycerol while regular stirring at 1000rpm for about 2-3 hours at 45 ±2 °C. After that, when a uniform gel was formed, 5mL of fluticasone propionate-loaded CSNPs were added to the gel. The homogenized gel was sonicated for 1 hour to remove all bubbles. Blank and drug-loaded formulations were poured separately into Petri dishes and incubated in an oven at 45 °C for 48 hours. The dried films were obtained and kept in a desiccator at 30-35 °C until further analysis.

Appearance and thickness

Films were weighed and their thickness measured with a digital micrometre to standardise the treatment. Five measurements were made from different areas of the film. Three readings of each size were recorded, corresponding to the standard deviation (±SD).

Morphology of films

The morphology of the drug-loaded nanofilm was evaluated using a Dino-Lite® microscope (Courage and Khazaka Electronic GmbH, Germany), a sophisticated digital light microscope.

FTIR analysis

FTIR analysis of the nanofilm and its components was achieved by the spectrophotometer (Perkin Elmer Spectrum 100 FTIR Spectrometer, USA) incorporated with an Attenuated Total Reflection (ATR) assembly. The FTIR

spectra were recorded for the pure drug, the blank, and the drug-loaded films in the range of 4000 to 550 cm-1 at a constant resolution of 2 cm-1. The dry film was cut into small pieces and placed on an ATR crystal.

In-vitro drug Release study

An *in-vitro* drug permeation study was conducted using a jacketed Franz-diffusion cell (Permegear Inc., USA) having a permeation area of 0.634 cm^2 and a 5 mL capacity of receptor cell volume with constant stirring speed (600 rpm) at 37±2°C. The PBS was used as the dissolution medium in the receiver compartment, with a final adjusted pH of 7.4±0.2 to simulate a chronic wound environment. A cellulose acetate membrane (0.45 µ) was used (Hussain *et al*., 2024). The nanofilm with a diameter of 2.1 cm was placed over the cellulose acetate membrane. The nanofilm diameter was selected to be larger to ensure the receptor is fully covered, leaving no area of the Franz-diffusion cell uncovered. Aliquots of the sample (0.5 mL) were collected at predetermined intervals, and an equal volume of fresh medium at 37 °C was added to maintain the standard volume of the receptor compartment. The concentration of the fluticasone propionate in the samples was evaluated using a UV-visible spectrophotometer (UV-1601, Shimadzu, Kyoto, Japan) at 246 nm.

In-vivo drug permeation study

Animal care and dosing

The Institutional Animal Care and Use Committee of the University of Veterinary and Animal Sciences approved experimental protocols for the use of animals UVAS/219.0A/17. Albino Wistar rats were included in this study. Animal care and treatment were conducted in accordance with the standard laboratory guidelines. Adult male Albino Wistar rats (~9 weeks old) were housed individually for 7 days under a precise environment (22 ± 3 ºC, 40-70% relative humidity, 12 h light/dark).

Dermal application

To determine the concentration of fluticasone propionate throughout the stratum corneum (SC) following film application, the skin was progressively removed using the standard tape-stripping method (Nagelreiter *et al*., 2015). Animals were divided into two groups: one drug loaded in NPs loaded film and 2nd group with a free form of film (without NPs). The skin sampling site was outlined to leave an exposed skin area for the SC, which was larger than that of the treated formulation. The dorsal skin area was shaved 12 hours before the treatment. Films were removed after 12 hours, and the area was swabbed with normal saline to remove any drug residue. The animals were anesthetized after intraperitoneal injections of Ketamine (60mg/kg) (Singh and Chandra, 2025). The area was dried before tape stripping began. With each stripping, SC is removed from the skin. After every interval, the tape stripping was done. This meant that a concentration of fluticasone propionate across the skin barrier could be achieved relative to the SC depth. Tapes collected at different times were placed in eluent (PBS, pH=7.4) to extract the drug in a mechanical shaking water bath at 37 ± 3 ºC for 6 hours. The eluent was analyzed using a UV spectrophotometer (λmax = 246 nm) to measure the concentration-time profile. Maximum drug concentration in the SC (C_{max}) and time to reach the maximum drug concentration (T_{max}) were determined. The linear trapezoidal rule was used to measure the area under the curve from 0 to 48 h (AUC 0-48 h).

Statistical analysis

Each experiment was replicated at least 3 times, and data were reported as mean ± SD. Statistical differences were determined by ANOVA followed by post hoc Tukey's test using GraphPad version 5.1 (GraphPad Software Inc., La Jolla, CA).

RESULTS

Preparation of fluticasone propionate NPs

LMW chitosan is a cationic polymer obtained from crab shells by deacetylation. NPs were formed when a negatively charged TPP solution was added to the CS solution in an acidic medium (pH 4.0-5.0).

Nanoparticle characterization

Fluticasone propionate loaded CS NPs were characterised by particle size and distribution. The average particle size of drug-loaded NPs was 250±4nm. The surface charge was +32.4 ± 1.5 mV, with a PDI of 1.112 ± 0.01. The NPs' size, shape, and surface charge are important physicochemical properties because they influence cellular uptake. The NPs' size was within the acceptable range, with a diameter of 257 ± 4 nm and a narrow size distribution in dynamic light scattering data (Fig. 1).

Scanning electron microscopy

The NPs shape was spherical with a smooth surface in SEM (Fig. 1). The particle size range in SEM was 250-260 ± 3nm, which was corroborated by zeta-sizer analysis.

Calibration curve

A serial dilution of the stock solution of fluticasone propionate was prepared, and the standard calibration curve was drawn against different absorbance values following Beer's Lambert Law. Fig. 2 indicates the standard calibration curve of the sample.

Drug loading and entrapment efficiency

The percentage of both drug loading capacity and entrapment efficiency was measured using a UV spectrophotometer (Shimadzu UV-1601, Kyoto, Japan) at 246 nm. As stated previously, the standard curve of fluticasone propionate was first determined to calculate the drug concentration in both supernatant (after ultracentrifuge) and NPs fraction (R2=0.997), as shown in Fig. 2. The drug loading and entrapment efficiency were 16.7 ± 0.8 % and 89.4 ± 3.6%, respectively (Table 1).

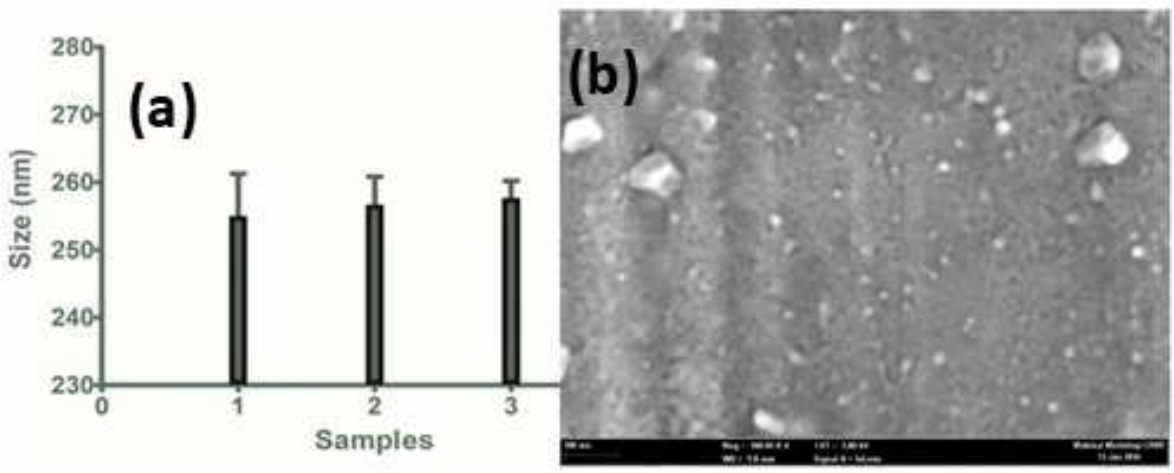

Fig. 1: Size (a) and shape of surface morphology (b) of the fluticasone propionate-loaded CS NPs.

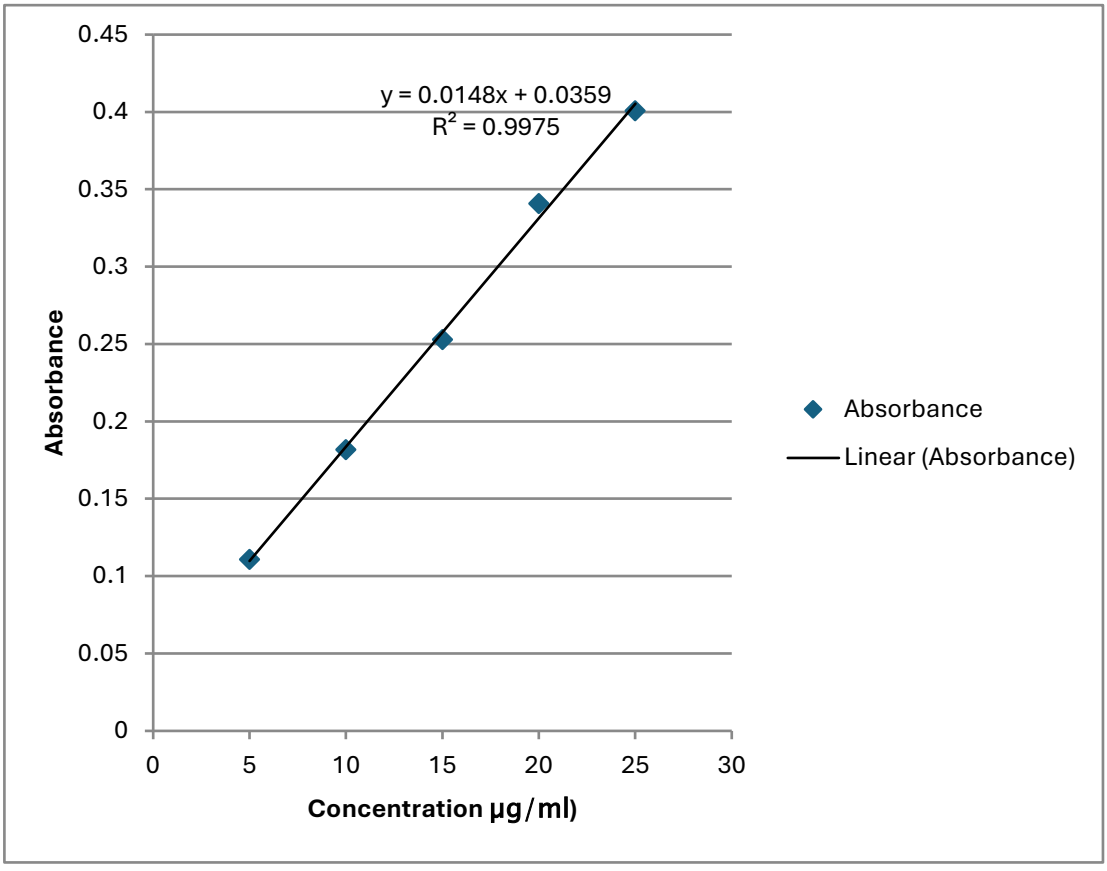

Fig. 2: Standard calibration curve of Fluticasone propionate.

Table 1: (a) Loading amount of PTX in nanoparticles was measured using a UV-spectrophotometer; (b) Loading efficiency of Fluticasone Propionate in nanoparticles was calculated from the ratio of loading content of drug/feed amount of drug in the nanoparticles; (c) The average size of each nanoparticle (1 mg/ml in PBS at 37 °C) was measured using dynamic light scattering.

Fluticasone propionate CSNPs	Size (nm)	PDI	Drug loading %	Entrapment efficiency %
	257 ± 4.6	1.112 ± 0.01	16.7 ± 0.8	89.4 ± 3.6

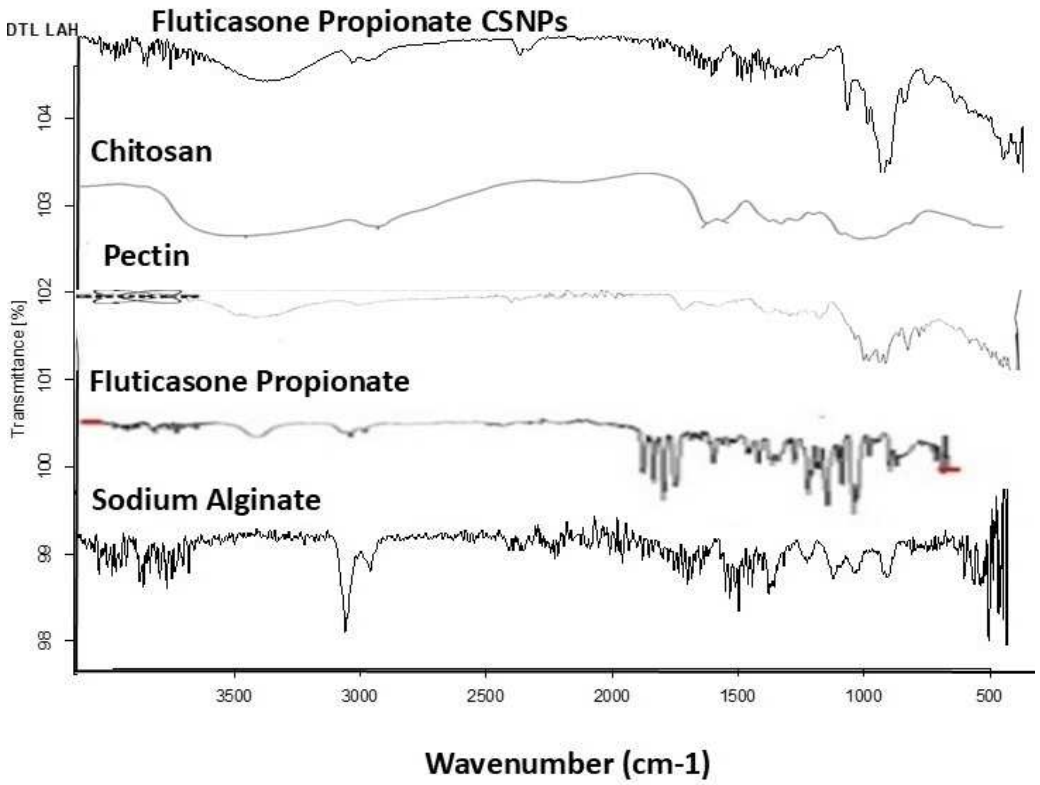

Fig. 3: FTIR spectra of blank sodium alginate, fluticasone propionate, pectin, chitosan, and fluticasone propionate loaded chitosan NPs.

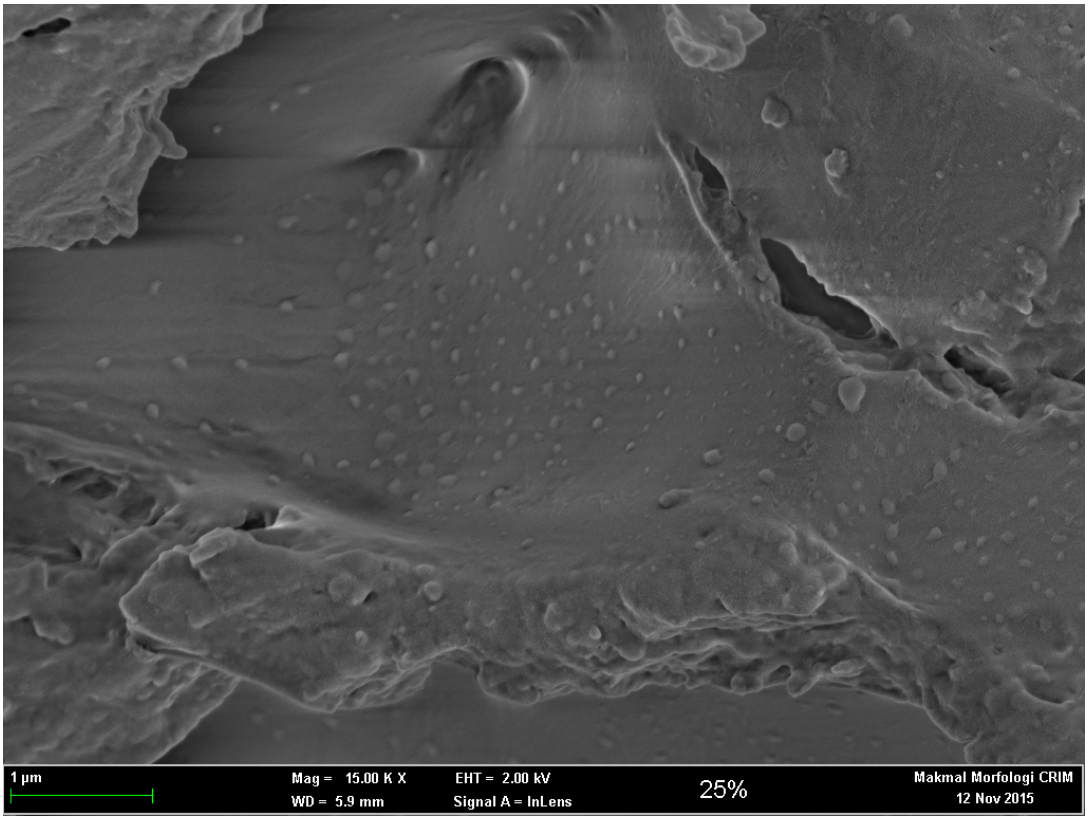

Fig. 4: Scanning electron microscopy images of the fluticasone propionate-loaded chitosan NPs-loaded film.

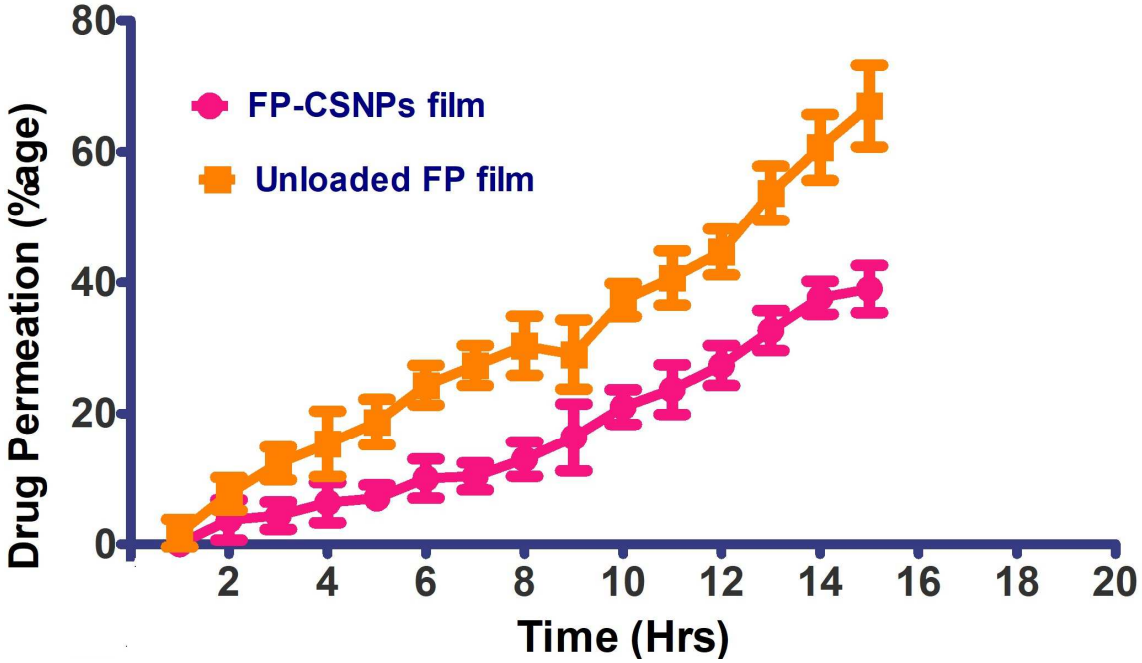

Fig. 5: Permeation profile of the fluticasone propionate, free and loaded in CSNPs.

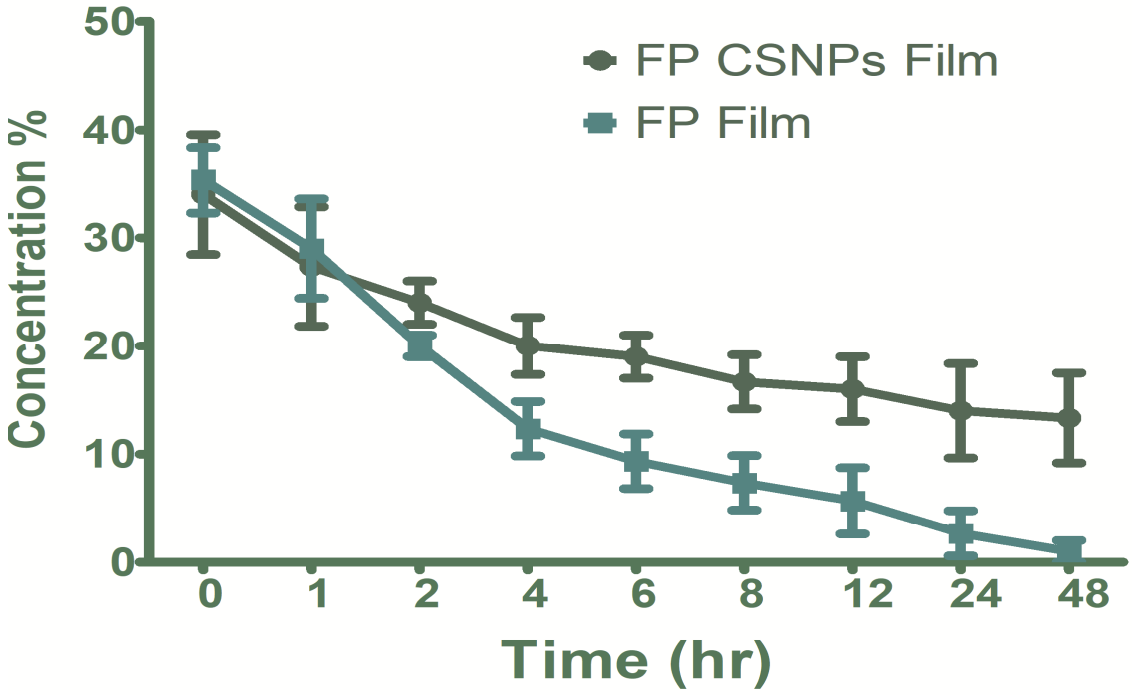

Fig. 6: Fluticasone Propionate loaded CSNPs film depth profile across the stratum corneum.

Fourier transform infrared spectroscopy analysis

Fig. 3 shows that FTIR analysis was employed to evaluate the interaction between polymers and drug molecules (Fluticasone propionate). The results indicate that the drug has been successfully loaded into the NPs and that there is no interaction between the drug molecule and other formulation components.

Scanning electron microscopy of the film

SEM was used to assess the film's exterior morphology. The result indicates the surface's smoothness (Fig. 4).

In-vitro drug release study

Franz diffusion is one of the simplest and well-established methods for studying drug permeation. The in vitro drug

permeation profile over time is shown in Fig. 5. Decreasing particle size increases the permeation flux through the skin.

In-vivo drug permeation study

In-vivo bioavailability studies in rats were conducted to evaluate the drug permeation across the skin. I*n in vitro and In-vivo co-relationships,* it is necessary to perform drug permeation through the animal skin. We use the standard Tape-stripping method to evaluate the drug diffusion behaviour through the rat skin model (Lademann *et al*., 2009; Siddique *et al*., 2016). Strips were collected at regular intervals. Animals were divided into two groups: Group 1, drug-loaded into a CSNPs film; and Group 2, a free-form film (without NPs). After continuous tape stripping, going deep down into the SC, about 16% of the drug is found as compared to the free form of the drug, where there is no penetration of the drug (Fig. 6).

DISCUSSION

The fabrication of CSNPs majorly depends on interactions of the positively charged NH^{3+} group in CS and the negatively charged TPP solution, by the formation through this ionic-gelation method, and entirely depends on the concentration of the free amino group present in CS (Ayumi *et al*., 2019; Takeuchi *et al*., 2001). The NPs' size, shape, and surface charge are important physicochemical properties as they influence the cellular uptake. The size of the nanoparticles also affects their penetration into the cellular appendages (Voigt *et al*., 2014). The NPs' size was within the acceptable range, with a size of 257 ± 4.6 nm and a narrow size distribution in dynamic light scattering data (Fig. 1). Regarding stability, the NPs' suspension depends on the surface potential (Wu *et al*., 2023). NPs remain distributed stably when they carry a surface charge, which causes electrostatic repulsion between them (Müller *et al*., 2001). Zeta potential and PDI were found to be in the acceptable limit range of NPs. NPs with higher surface charge are responsible for the increase in zeta potential because of the higher repulsive forces between the particles, ultimately preventing them from aggregating (Ibrahim *et al*., 2023). The cationic charge on the CS surface also shows a key role in its attachment to the cell. It has been reported that CS increases skin penetration by interacting with the tight junctions of the epidermis (Ma *et al*., 2022). The size of the nanoparticles also affects their penetration into the cellular appendages (Voigt *et al*., 2014). As in earlier studies, CS shows a distinct peak at 3438.3 cm^{-1} (Ullah *et al*., 2022). Fluticasone propionate shows distinct peaks at 1890.5 cm^{-1}. In CS spectra, the amide I and amide II bending vibrations shifted from 1689.1 and 1618.01 to 1628.01 and 1498.1 cm−1, indicating a relationship among the NH3+ functional groups of CS, TPP, and drugs within the Fluticasone propionate CSNPs range. It has been shown that particle size plays a significant role in drug permeation through the skin (Oktay *et al*., 2021). The slow release of Fluticasone propionate is due to swelling and erosion (Ahmady *et al*., 2022). First, swelling occurs when water penetrates the matrix, making the polymer rubbery and susceptible to degradation (Cardoso *et al*., 2019). Fluticasone propionate-loaded NPs showed a better release profile than the free form (Fig. 5). Controlled release of the fluticasone propionate from the CSNP film indicates that it will stay over the application area for about 40% release in 16 hours.

The ability of a topically applied NPs-loaded film depends on the function of drug retention in the application area (Lunter *et al*., 2024). Whereas more than 70% of the drug release from the unloaded film dosage form (Fig. 5). The result showed that drug release from the unloaded formulation was significantly higher than the NPs loaded formulation ($p<0.05$). The lower release rate of the polymeric NPs-loaded film compared to the formulation without NPs indicates NP inclusion in the film blend (Tufail *et al*., 2022; Arezomand *et al*., 2024). In this *in-vivo* dermal pharmacokinetic study, the SC level of a drug is more relevant to local dermatological efficacy than its plasma concentration. (Abuelella *et al*., 2023; Ta *et al*., 2021). The results indicate that penetration of the drug-loaded CSNPs is much higher compared to the free form of the drug (Lee *et al*., 2019). The *in-vitro, in-vivo* correlation indicates that the CSNPs-loaded formulation increases the rate of drug penetration through the skin and maintains the drug's sustained release mechanism. It signifies that CSNPs may act as a depot and deliver Fluticasone propionate in a sustained manner (Ta *et al*., 2021). Moreover, this relationship indicates that the percentage of drug permeation and the percentage of drug absorbed through the skin showed a point-to-point regression. Hence, the *in-vitro* drug permeation study is not statistically significant ($p>0.05$) compared with the *in-vivo* permeation study.

CONCLUSION

Fluticasone propionate-loaded CSNPs were magnificently assembled by the ionic-gelation method. The results showed key NP characteristics, including particle size, zeta potential, and surface morphology. The formation of NPs and the interaction of the polymers with drug molecules were confirmed by the FTIR. Surface morphology was examined using SEM. Drug release study indicating higher skin permeation. Overall, the results indicate that a CSNP-loaded film can enhance the skin permeation and bioavailability of fluticasone propionate.

Acknowledgment

The authors extend their appreciation to the Deanship of Scientific Research at Northern Border University, Arar, KSA, for funding this research work through the project number "NBU-FFR-2025-3336-05.

Author contributions

MIS: Writing the original draft, review and editing validation, Formal analysis, conceptualization, Investigation, Project administration, and supervision.

Funding
There is no funding for the following project.

Data availability statement
All data generated or analysed during this study are included in this published article and its supplementary information files. Only use this if all data is in the manuscript or supplementary files.

Ethical approval
The Committee of the University of Veterinary and Animal Sciences approved experimental protocols for the use of animals UVAS/219.0A/17.

Conflict of interest
The author declares no conflict of interest.

REFERENCES

Abdel-mottaleb MM, Moulari B, Beduneau A, Pellequer Y and Lamprecht (a. 2012). Nanoparticles enhance therapeutic outcome in inflamed skin therapy. *Eur. J. Pharm. Biopharm.,* **82**(1): 151-157.

Abuelella KE, Abd-allah H, Soliman SM and Abdel-mottaleb MM (2023). Skin targeting by chitosan/hyaluronate hybrid nanoparticles for the management of irritant contact dermatitis: *In-vivo* therapeutic efficiency in mouse-ear dermatitis model. *Int. J. Biol. Macromol.,* **232**: 123458.

Ahmady AR, Razmjooee k, Saber-Samandari S and Toghraie D (2022). Fabrication of chitosan-gelatin films incorporated with thymol-loaded alginate microparticles for controlled drug delivery, antibacterial activity and wound healing: *in-vitro* and *in-vivo* studies. *Int. J. Biol. Macromol.,* **223**(Part A): 567-582.

Almawi WY and Melemedjian OK (2002). Molecular mechanisms of glucocorticoid antiproliferative effects: Antagonism of transcription factor activity by glucocorticoid receptor. *J. Leukocyte Biol.,* **71**(1): 9-15.

Arezomand Z, Mashjoor S, Makhmalzadeh BS, Shushizadeh MR and Khorsandi L (2024). Citrus flavonoids-loaded chitosan derivatives-route nanofilm as drug delivery systems for cutaneous wound healing. *Int. J. Biol. Macromol.,* **271**: 132670.

Ashraf M, El-Sawy HS, El Zaafarany GM and Abdel-Mottaleb MM (2025). Eucalyptus oil nanoemulsion for enhanced skin deposition of fluticasone propionate in psoriatic plaques: A combinatorial anti-inflammatory effect to suppress implicated cytokines. *Arch. Pharm.,* **358**(1): e2400557.

Ayumi NS, Sahudin S, Hussain Z, Hussain M and Samah NHA (2019). Polymeric nanoparticles for topical delivery of alpha and beta arbutin: Preparation and characterization. *Drug Deliv Transl Res,* **9**(2): 482-496.

Cardoso AM, De Oliveira EG, Coradini k, Bruinsmann FA, Aguirre T, Lorenzoni R, Barcelos RCS, roversi k, Rossato DR and Pohlmann AR (2019). Chitosan hydrogels containing nanoencapsulated phenytoin for cutaneous use: skin permeation/penetration and efficacy in wound healing. M*ater. Sci. Eng. C,* **96**: 205-217.

Deb A, Mandurnekar AA, Rani V, Chauhan T, Mishra B and Chawla R (2018). Formulation and evaluation of curcumin loaded nanofilms for the treatment of wounds. S*per J. of Pharm. and Biol. Res.,* **1**: 5-9.

Delouise LA (2012). Applications of nanotechnology in dermatology. *J. Invest. Dermatol.,* **132**(3): 964-975.

Gan Q and Wang T (2007). Chitosan nanoparticle as protein delivery carrier-systematic examination of fabrication conditions for efficient loading and release. *Colloids Surf., B.,* **59**(1): 24-34.

Hussain A, Altamimi MA and Alneef YS (2024). Hspip and QBD oriented optimized stearylamine-elastic liposomes for topical delivery of ketoconazole to treat deep seated fungal infections: *In-vitro* and *ex-vivo* evaluations. *Int. J. Pharm., X.,* **8**: 100279.

Ibrahim MA, Alhalafi MH, Emam EAM, Ibrahim H and Mosaad RM (2023). A review of chitosan and chitosan nanofiber: preparation, characterization and its potential applications. *Polymers,* **15**(13): 2820.

Illum l (2007). Nanoparticulate systems for nasal delivery of drugs: A real improvement over simple systems? *J. Pharm. Sci.,* **96**(3): 473-483.

Korting H and Schollmann C (2012). Topical fluticasone propionate: Intervention and maintenance treatment options of atopic dermatitis based on a high therapeutic index. *J Eur Acad Dermatol Venereol,* **26**(2): 133-140.

Kulkarni RR, Phadtare DG and Saudagar RB (2016). UV spectrophotometric method development and validation of fluticasone propionate. A*sian J. Pharm. Sci.,* **6**(2): 135-138.

Lademann J, Jacobi U, Surber C, Weigmann HJ and Fluhr J (2009). The tape stripping procedure–evaluation of some critical parameters. *Eur. J. Pharm. Biopharm.,* **72**(2): 317-323.

Lee JS, Hwang Y, Oh H, Kim S, Kim JH, Lee JH, Shin YC, Tae G and Choi WI (2019). A novel chitosan nanocapsule for enhanced skin penetration of cyclosporin A and effective hair growth *In-vivo*. N*ano Res.,* **12**(12): 3024-3030.

Lunter D, Klang V, Eichner A, Savic SM, Savic S, Lian G and Erdo F (2024). Progress in topical and transdermal drug delivery research-focus on nanoformulations. *Pharmaceutics,* **16**(6): 817.

Ma J, Wang Y and Lu R (2022). Mechanism and application of chitosan and its derivatives in promoting permeation in transdermal drug delivery systems: A review. *Pharmaceuticals,* **15**(4): 459.

Müller R, Jacobs C and Kayser O (2001). Nanosuspensions as particulate drug formulations in therapy: Rationale for development and what we can expect for the future. *Adv. Drug Delivery Rev.,* **47**(1): 3-19.

Nagelreiter C, Mahrhauser D, Wiatschka K, Skipiol S and Valenta C (2015). Importance of a suitable working protocol for tape stripping experiments on porcine ear

skin: influence of lipophilic formulations and strip adhesion impairment. *Int. J. Pharm.,* **491**(1-2): 162-169.

Nutten S (2015). Atopic dermatitis: Global epidemiology and risk factors. *Ann. Nutr. Metab.,* **66**(Suppl. 1): 8-16.

Oktay AN, Ilbasmis-Tamer S, Uludag O and Celebi N (2021). Enhanced dermal delivery of flurbiprofen nanosuspension based gel: Development and ex vivo permeation, pharmacokinetic evaluations. *Pharm. Res.,* **38**(6): 991-1009.

Papadimitriou S, Bikiaris D, Avgoustakis K, Karavas E and Georgarakis M (2008). Chitosan nanoparticles loaded with dorzolamide and pramipexole. *Carbohydr. Polym.,* **73**(1): 44-54.

Parhi R, Suresh P and Patnaik S (2015). Physical means of stratum corneum barrier manipulation to enhance transdermal drug delivery. *Curr. Drug Delivery,* **12**(2): 122-138.

Pati F, Adhikari B and Dhara S (2011). Development of chitosan–tripolyphosphate fibers through pH dependent ionotropic gelation. *Carbohydr. Res.,* **346**(16): 2582-2588.

Siddique MI, Katas H, Amin MCIM, Ng SF, Zulfakar MH, Buang F and Jamil A (2015). Minimization of local and systemic adverse effects of topical glucocorticoids by nanoencapsulation: *In-vivo* safety of hydrocortisone–hydroxytyrosol loaded chitosan nanoparticles. J. *Pharm. Sci.,* **104**(12): 4276-4286.

Siddique MI, Katas H, Amin MCIM, Ng SF, Zulfakar MH and Jamil A (2016). *In-vivo* dermal pharmacokinetics, efficacy and safety of skin targeting nanoparticles for corticosteroid treatment of atopic dermatitis. *Int. J. Pharm.,* **507**(1-2): 72-82.

Singh N and Chandra P (2025). Evaluation of in vitro antioxidant activity of chrysin and *In-vivo* wound healing potential of an optimized chrysin emulgel formulation. *J Biomater Sci Polym Ed*, 1-16.

Sivakumar S, Safhi MM, Aamena J and Kannadasan M (2013). Pharmaceutical Aspects of Chitosan Polymer "in brief". *Res J Pharm Tech,* **6**(12): 1439-42.

Ta Q, Ting J, Harwood S, Browning N, Simm A, Ross K, Olier I and Al-kassas R (2021). Chitosan nanoparticles for enhancing drugs and cosmetic components penetration through the skin. *Eur. J. Pharm. Sci.,* **160**: 105765.

Takeuchi H, Yamamoto H and Kawashima Y (2001). Mucoadhesive nanoparticulate systems for peptide drug delivery. *Adv. Drug Delivery Rev.,* **47**(1): 39-54.

Try C, Moulari B, Beduneau A, Fantini O, Pin D, Pellequer Y and Lamprecht A (2016). Size dependent skin penetration of nanoparticles in murine and porcine dermatitis models. *Eur. J. Pharm. Biopharm.,* **100**: 101-108.

Tufail S, Siddique MI, Sarfraz M, Sohail MF, Shahid MN, Omer MO, Katas H and Rasool F (2022). Simvastatin nanoparticles loaded polymeric film as a potential strategy for diabetic wound healing: *In vitro* and *in-vivo* evaluation. C*urr. Drug Delivery,* **19**(5): 534-546.

Ullah S, Azad AK, Nawaz A, Shah KU, Iqbal M, Albadrani GM, Al-joufi FA, Sayed AA and Abdel-daim MM (2022). 5-fluorouracil-loaded folic-acid-fabricated chitosan nanoparticles for site-targeted drug delivery Cargo. *Polymers,* **14**(10): 2010.

Voigt N, Henrich-noack P, Kockentiedt S, Hintz W, Tomas J and Sabel BA (2014). Toxicity of polymeric nanoparticles *In-vivo* and *in-vitro*. J. *Nanopart. Res.,* **16**(6): 2379.

Wu Y, Gao H, Liu J and Liang H (2023). Chitosan nanoparticles efficiently enhance the dispersibility, stability and selective antibacterial activity of insoluble isoflavonoids. *Int. J. Biol. Macromol.,* **232**: 123420.

Yassin AEB, Anwer MK, Mowafy HA, El-bagory IM, Bayomi MA and Alsarra IA (2010). Optimization of 5-fluorouracil solid-lipid nanoparticles: A preliminary study to treat colon cancer. *Int. J. Med. Sci.,* **7**(6): 398.